

3M-Diffusion: Latent Multi-Modal Diffusion for Text-Guided Generation of Molecular Graphs

Huaisheng Zhu^{*1} Teng Xiao^{*1} Vasant G Honavar¹

Abstract

Generating molecules with desired properties is a critical task with broad applications in drug discovery and materials design. Inspired by recent advances in large language models, there is a growing interest in using natural language descriptions of molecules to generate molecules with the desired properties. Most existing methods focus on generating molecules that precisely match the text description. However, practical applications call for methods that generate diverse, and ideally novel, molecules with the desired properties. We propose 3M-Diffusion, a novel multi-modal molecular graph generation method, to address this challenge. 3M-Diffusion first encodes molecular graphs into a graph latent space aligned with text descriptions. It then reconstructs the molecular structure and atomic attributes based on the given text descriptions using the molecule decoder. It then learns a probabilistic mapping from the text space to the latent molecular graph space using a diffusion model. The results of our extensive experiments on several datasets demonstrate that 3M-Diffusion can generate high-quality, novel and diverse molecular graphs that semantically match the textual description provided. Code is released at <https://github.com/huaishengzhu/3MDiffusion>.

1. Introduction

Generating molecules with the desired properties is a critical task with broad applications in drug discovery and materials design (Hajduk & Greer, 2007; Mandal et al., 2009; Pyzer-Knapp et al., 2015). There is a growing interest in generative models to automate this task (You et al., 2018; Jin et al., 2018; 2020; Bjerrum & Threlfall, 2017). Kusner et al. (2017) proposed a variational autoencoder that

^{*}Equal contribution ¹The Pennsylvania State University, USA. Correspondence to: Huaisheng Zhu <hvz5312@psu.edu>, Teng Xiao <tengxiao@psu.edu>, Vasant Honavar <vuh14@psu.edu>.

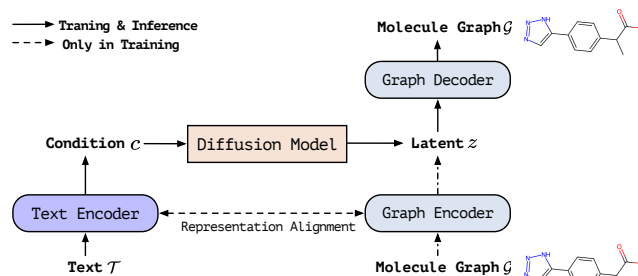


Figure 1. The overview of 3M-diffusion, with a molecule graph encoder/decoder and a latent diffusion model conditioned on a prior (an aligned text encoder). The details of alignment in the text/graph encoders and diffusion model are given in Section 4.

uses parse trees for probabilistic context free grammars to encode discrete sequences that specify the Simplified Molecular-Input Line-entry System (SMILES) (Weininger, 1988) notation of molecules use the resulting parse trees to generate SMILES codes that describe molecular graphs. Edwards et al. (2021) formulated molecule retrieval from textual description as a cross-lingual retrieval task. Recent advances in language models have led to innovative approaches to generate molecules from human-friendly textual descriptions of their properties, substructures, and biochemical activity (Edwards et al., 2022; Zeng et al., 2022; Zhao et al., 2023b; Fang et al., 2023a). These approaches learn mappings from textual descriptions to chemical structures using single transformer-based cross-lingual language model for molecule generation. Specifically, with the given text description of the molecule, these approaches produce SMILES strings describing the molecular graph.

Despite promising initial results, such approaches suffer from some important limitations: (i) SMILES encoding is degenerate in that the a given molecular graph can have multiple SMILE encodings. For example, the structure of ethanol can be specified using CCO, OCC or C(O)C. Although a unique canonical SMILES representation can be produced for a given graph, the procedure used to do so relies on several arbitrary choices. Not surprisingly, molecules with identical chemical graphs may map to significantly distinct SMILES strings, making SMILES notation less than ideal for generating molecules from their textual descriptions (Jin et al., 2018). Important chemical properties

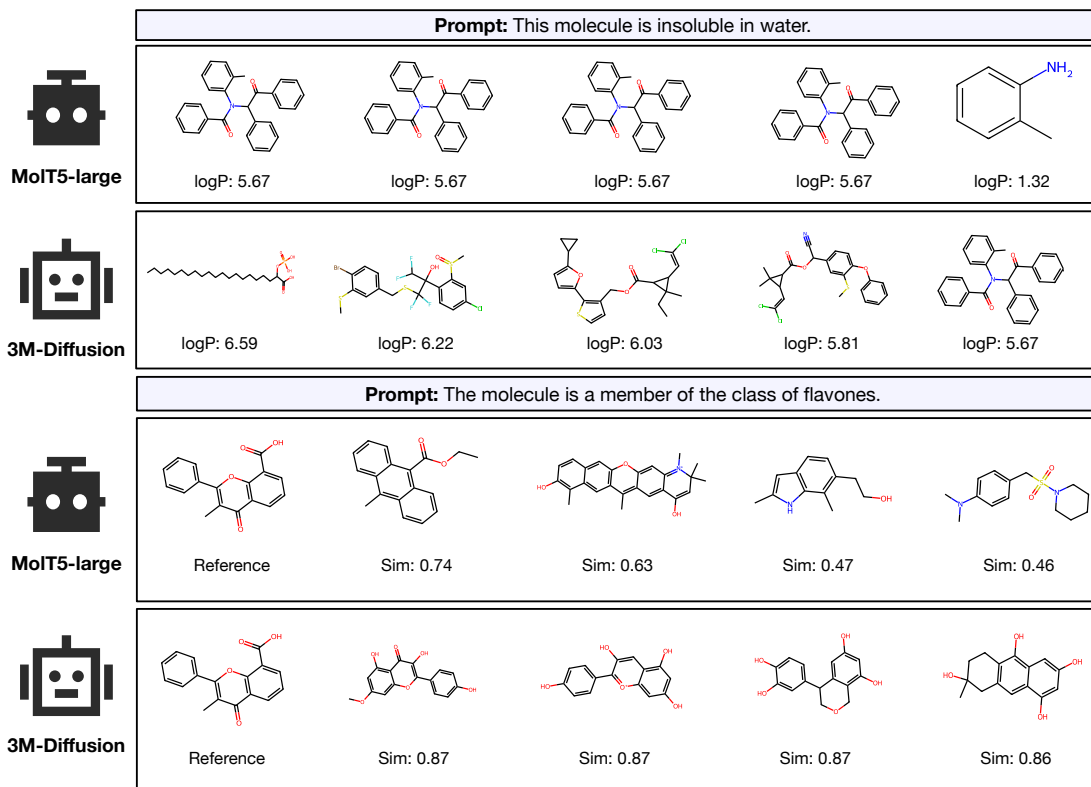


Figure 2. Qualitative comparisons to the MolT5-large in terms of generated molecules on ChEBI-20. Compared with the SOTA method MolT5-large, our generated results are more diverse and novel with maintained semantics in textual prompt.

corresponding to the substructures of molecules are more straightforward to express using molecular graphs rather than linear SMILES representations (Jin et al., 2018; Du et al., 2022); (ii) Using language models to generate diverse high-quality molecules matching a description is challenging, because the decoding process used such as beam search or greedy search often produces candidates that are often too similar to each other as shown in Figure 2. Hence, there is an urgent need for better approaches to generating diverse, novel molecular graphs from a given textual description (Brown et al., 2019). Against this background, this paper aims to answer the following research question: *How can we generate a diverse and novel collection of molecular graphs that match a given textual description?*

In this work, we introduce 3M-Diffusion, a novel multimodal molecular diffusion method, for generating high-quality, diverse, novel molecular graphs given a textual description. Inspired by text-guided image generation using a diffusion model on the latent space (Rombach et al., 2022), 3M-Diffusion is trained to generate molecules from the latent distribution of a molecular graph autoencoder (See Figure 1). This enables the diffusion process to focus on the high-level semantics of molecules. We find that this approach is particularly well-suited for discrete molecular graph modality because it offloads the challenge of modeling a discrete and diverse distribution to the autoencoder

and simplifies the diffusion process by restricting it to the continuous, latent feature space. Since graph data consists of both node attributes and graph structure, which differs significantly from the sequential and contextual nature of text data, to align the latent space of the text and molecular graph, 3M-diffusion first pretrains molecular graph and text encoders through contrastive learning on a large dataset of molecule-text pairs, enabling generate high-quality molecular graphs that match the given textual descriptions. Our extensive experiments demonstrate that 3M-Diffusion can generate high-quality, novel, and diverse molecular graphs that semantically match the textual description provided.

Key Contributions. The key contributions of this paper are as follows: (i) To the best of our knowledge, 3M-Diffusion offers the first multimodal diffusion approach to generating molecular graphs from their textual descriptions, surpassing the limitations of state-of-the-art (SOTA) methods for this problem. (ii) 3M-Diffusion aligns the latent spaces of molecular graphs and textual descriptions to offer a text-molecule aligned latent diffusion model to generate higher-quality, diverse, and novel molecular graphs that match the textual description provided; and (iii) We present results of extensive experiments using four real-world text-based molecular graphs generation benchmarks that show that 3M-Diffusion outperforms SOTA methods for both text-guided and unconditional molecular graph generation. In particular,

3M-Diffusion achieves 146.27% novelty, 130.04% diversity relative improvement over the SOTA method with maintained semantics in textual prompt on the PCDes dataset.

2. Related Work

2.1. Molecule Generation

Existing molecular graph generation methods can be broadly grouped into two categories: text-based and graph-based models. Text-based models typically utilize the SMILES (Weininger, 1988) or SELFIES (Krenn et al., 2022) linear strings to describe each molecule (Bjerrum & Threlfall, 2017; Gómez-Bombarelli et al., 2018; Kusner et al., 2017; Flam-Shepherd et al., 2022; Fang et al., 2023b; Grisoni, 2023). Because a given molecular graph can have several linear string representations and slight changes to the string representation can yield significant changes in molecular graph being described, such linear string encodings are far from ideal for learning generative models for producing molecular graph from textual descriptions, several authors have used deep generative models, including graph variational autoencoders (VAEs) (You et al., 2018; Jin et al., 2018; Xiao et al., 2021; Jin et al., 2020; Kong et al., 2022; Liu et al., 2018; Diamant et al., 2023), normalizing flows (Madhawa et al., 2019; Zang & Wang, 2020; Luo et al., 2021), generative adversarial networks (Guarino et al., 2017; Maziarka et al., 2020), diffusion models (Niu et al., 2020; Vignac et al., 2022; Jo et al., 2022) and autoregressive models (You et al., 2018; Xiao & Wang, 2021; Popova et al., 2019; Goyal et al., 2020) to learn distributions of molecular graphs from large databases of known graphs. However, many of these studies focus on generating molecular graphs with specified low-level properties, such as logP (the octanol-water partition coefficient) as opposed to those that match high-level textual descriptions of molecules (Edwards et al., 2022). However, practical applications, such as drug design, call for effective approaches to generating diverse and novel molecular graphs that match a given textual description.

2.2. Text-guided Generation of Molecular Graphs

Advances in deep learning and language models have inspired a growing body of work on applications of such models to problems in the molecular sciences (Schwaller et al., 2019; Xiao et al., 2023; Toniato et al., 2021; Xiao et al., 2024; Zhao et al., 2023a; Seidl et al., 2023; Schwaller et al., 2021; Vaucher et al., 2020). Advances in text-guided generation of images, videos, and audios (Radford et al., 2021; Rombach et al., 2022; OpenAI, 2023; Yin et al., 2023), together with the flexibility offered by natural language descriptions of molecular graphs have inspired a growing body of work on text-guided generation of molecular graphs (Christofidellis et al., 2023; Edwards et al., 2022; Fang et al., 2023a; Zeng et al., 2022; Su et al., 2022). For

example, MolT5 (Edwards et al., 2021; 2022) and ChemT5 (Christofidellis et al., 2023) pre-train on a substantial volume of unlabeled language text and SMILES strings for tasks such as molecule captioning and text-based molecule generation (Christofidellis et al., 2023; Edwards et al., 2022). However, as noted above, the degenerate nature of linear SMILES string representation of molecular graphs makes it less ideal for generating molecules from their textual descriptions. To address this problem, we propose 3M-Diffusion, aligning latent representations of textual descriptions for molecules with the latent representations of the graphs themselves, offering a powerful approach for text-guided molecule generation.

3. Preliminaries

3.1. Problem Definition

In this paper, we consider generative modeling of 2D molecular graphs from scratch. Each molecule is represented as a graph $\mathcal{G} = (\mathcal{V}, \mathcal{E})$, where $\mathcal{V} = \{v_1, \dots, v_{|\mathcal{V}|}\}$ is the set of $|\mathcal{V}|$ nodes and \mathcal{E} is the set of edges. Let $\mathbf{X} = [\mathbf{x}_1, \mathbf{x}_2, \dots, \mathbf{x}_{|\mathcal{V}|}] \in \mathbb{R}^{|\mathcal{V}| \times D_x}$ be the node attribute matrix, where x_i is the D_x -dimensional one-hot encoding feature vector of v_i , such as atomic type and chirality type. Similarly, a tensor $\mathbf{A} \in \mathbb{R}^{|\mathcal{V}| \times |\mathcal{V}| \times b}$ groups the one-hot encoding e_{ij} of each edge, with each entry representing a distinct edge type (bond types for molecule), while treating the absence of an edge as a specific edge type. Given the dataset $\mathcal{D} = \{(\mathcal{G}_i, \mathcal{T}_i)_{i=1}^N\}$ where molecule \mathcal{G} has specific text descriptions \mathcal{T} characterizing the features of the molecule, our goal is to learn conditional generation models $p_\theta(\mathcal{G} | \mathcal{T})$ for generating novel, diverse, and valid molecules while simultaneously aligning with the desired features outlined in text descriptions \mathcal{T} . For brevity, in what follows, we omit the input subscript i unless otherwise stated.

3.2. Diffusion Models

Diffusion models (DMs) (Ho et al., 2020; Song et al., 2020) are latent variable models that represent the data z_0 as Markov chains $\mathbf{z}_T \cdots \mathbf{z}_0$, where intermediate variables share the same dimension. DMs involve a forward diffusion process $q(\mathbf{z}_{1:T} | \mathbf{z}_0) = \prod_{t=1}^T q(\mathbf{z}_t | \mathbf{z}_{t-1})$ that systematically adds Gaussian noise to samples and a reverse process $p_\theta(\mathbf{z}_{0:T}) = p(\mathbf{z}_T) \prod_{t=1}^T p_\theta(\mathbf{z}_{t-1} | \mathbf{z}_t)$ that iteratively "denoises" samples from the Gaussian distribution to generate samples from the data distribution. A formal description of diffusion models is given in the Appendix A. To ensure training stability, we can use a simple regression objective with a denoising network $\hat{\mathbf{z}}_\theta$ with input (\mathbf{x}_t, t) :

$$\mathcal{L}_{\text{diff}} = \mathbb{E}_{t, \mathbf{x}_0, \epsilon} \left[\lambda_t \|\hat{\mathbf{z}}_\theta(\sqrt{\alpha_t} \mathbf{z}_0 + \sqrt{1 - \alpha_t} \epsilon, t) - \mathbf{z}_0\|_2^2 \right], \quad (1)$$

where t is the timestep, $\alpha_t \in [0, 1]$ is the noise schedule and $\epsilon \sim \mathcal{N}(\mathbf{0}, \mathbf{I})$ is Gaussian noise and λ_t is a time-dependent

weighting term. Intuitively, the denoising network is trained to denoise a noisy state, $\mathbf{z}_t = \sqrt{\alpha_t}\mathbf{z}_0 + \sqrt{1 - \alpha_t}\epsilon$, aiming to reconstruct the clean data \mathbf{z}_0 with Equation (1) that prioritizes specific times t . After training, we can draw samples with $\hat{\mathbf{z}}_\theta$ by the iterative ancestral sampling (Ho et al., 2020):

$$\begin{aligned} \mathbf{z}_{t-1} = & \frac{\sqrt{\alpha_{t-1}(1-\alpha_{t|t-1})}}{1-\alpha_t} \hat{\mathbf{z}}_\theta(\mathbf{x}_t, t) \\ & + \frac{\sqrt{\alpha_{t|t-1}(1-\alpha_{t-1})}}{1-\alpha_t} \mathbf{z}_t + \sigma(t-1, t)\epsilon, \end{aligned} \quad (2)$$

where $\alpha_{t|t-1}$ represents α_t/α_{t-1} and $\sigma(t-1, t) = (1 - \alpha_{t-1})(1 - \alpha_{t|t-1})/(1 - \alpha_t)$. The sampling chain is initialized from Gaussian prior $\mathbf{z}_T \sim p(\mathbf{z}_T) = \mathcal{N}(\mathbf{z}_T; \mathbf{0}, \mathbf{I})$.

4. Latent Multi-Modal Diffusion for Molecules

Our 3M-Diffusion in Figure 1 aims to learn a probabilistic mapping from the latent space of textual descriptions to a latent space of molecular graphs for text-guided generation of molecular graphs. However, direct mapping between these two latent representations using a diffusion model faces a key hurdle, namely, large mismatch between the latent spaces of textual descriptions and of molecular graphs. To overcome this hurdle, 3M-Diffusion adopts a two-part approach using a text-molecule aligned variational autoencoder and a multi-modal molecule latent diffusion. The former learns to align the representation of molecular graphs with that of their textual descriptions using contrastive learning, followed by a decoder that maps the latent representation back to the corresponding molecular graphs. The latter works with the text-aligned latent representation of molecular graphs to learn a conditional generative model, that maps textual descriptions to latent representations of molecular graphs. As we will see later, 3M-Diffusion is able to produce a diverse collection of novel molecular graphs that match the given textual descriptions.

4.1. Text-Molecule Aligned Variational Autoencoder

Our text-molecule aligned variational autonecoder comprises of three parts: the molecular graph encoder E_g , text encoder E_t and molecular graph decoder D . To bridge the representation gap between molecular graphs and their textual descriptions, the text and molecular graph encoders are trained on a large-scale dataset of molecule-text pairs. These encoders learn a well-aligned shared text-molecule representation, enriching the semantics of the molecular graph representation by aligning it the latent representation of textual descriptions of molecules through contrastive learning. These three parts are described in more detail below:

Molecular Graph Encoder aims to map each molecular graph \mathcal{G} with the adjacency tensor \mathbf{A} and node features matrix \mathbf{X} into a lower-dimensional latent space \mathcal{Z} . This transformation maps the discrete space of graph structures

and node attributes into a continuous latent space. Specifically, we use Graph Isomorphism Network (GIN) (Hu et al., 2019) as encoder network on the input adjacency tensor \mathbf{A} and node features \mathbf{X} of graph \mathcal{G} to derive the mean and standard deviation of the variational marginals:

$$\mu_g, \sigma_g = \text{GIN}(\mathbf{A}, \mathbf{X}), \quad (3)$$

where μ_g and σ_g represent the mean and standard deviations, respectively. Then, the latent graph representation \mathbf{z} is sampled from a Gaussian distribution as $\mathbf{z} \sim q(\mathbf{z} | \mathbf{A}, \mathbf{X}) \simeq \mathcal{N}(\mu_g, \sigma_g)$. This graph encoding process can also be expressed as $\mathbf{z} = E_g(\mathcal{G})$ signifying the outcome of the encoding operation within the input context of \mathcal{G} .

Text Encoder maps the textual descriptions of molecular graphs into a latent space, that provides input to a conditional generative model of molecular graphs. This encoded information becomes instrumental in generating molecules that match a given textual description. To inject potentially useful scientific knowledge from the literature into E_t we initialize it with Sci-BERT (Beltagy et al., 2019), an encoder-only transformer pretrained on scientific publications.

Aligning the representation of molecular graphs with that of their textual descriptions is crucial for establishing a shared representation for effective text-guided molecular graph generation. Graph data consists of both node attributes and graph structure, which differs significantly from the sequential and contextual nature of text data. We aim to align the molecule representation from the molecule graph encoder E_g with text representation from the text encoder E_t by pretraining. Consider a molecular graph \mathcal{G} and its textual description \mathcal{T} . To align these two encoders and ensure a cohesive latent space, we employ the following contrastive learning loss over a batch $\mathcal{B} \in \mathcal{D}$ of large-scale dataset containing molecule-text pairs to pretrain encoders:

$$\mathcal{L}_{\text{con}} = -\frac{1}{|\mathcal{B}|} \sum_{(\mathcal{G}_i, \mathcal{T}_i) \in \mathcal{B}} \log \frac{\exp(\cos(\mathbf{z}_i, \mathbf{c}_i)/\tau)}{\sum_{j=1}^{|\mathcal{B}|} \exp(\cos(\mathbf{z}_i, \mathbf{c}_j)/\tau)}, \quad (4)$$

where $\mathbf{z}_i = E_g(\mathcal{G}_i)$, $\mathbf{c}_i = E_t(\mathcal{T}_i)$ and $\mathbf{c}_j = E_t(\mathcal{T}_j)$ are representations of corresponding molecule graph and texts, respectively. $\cos(\cdot, \cdot)$ denotes cosine similarity and τ is the temperature hyperparameter. The encoders are pretrained on molecule-text (300K) pairs from PubChem collected by Liu et al. (2023) and robust enough to capture a well-aligned molecule-text space, which overcomes the challenges posed by the distribution gap and produce more consistent and high-quality results in cross-modal molecule generation.

Molecular Graph Decoder learns to use latent representation \mathbf{z} to decode the molecular graph. In this work, we employ the HierVAE (Jin et al., 2020) decoder, as it works empirically well in our final model. Note that our approach remains flexible and can be easily applied to other graph decoders (Li et al., 2018; Kong et al., 2022; Grover et al.,

2019). Specifically, it generates a molecule \mathcal{G} using a graph representation \mathbf{z} from the encoder. Given the molecular graph \mathcal{G} , we minimize the negative Evidence Lower Bound (ELBO) (Jin et al., 2020) to train both encoder and decoder:

$$\mathcal{L}_{\text{elbo}} = -\mathbb{E}_{q(\mathbf{z}|\mathbf{A},\mathbf{X})}[p(\mathcal{G}|\hat{\mathcal{G}})] + \alpha\text{KL}[q(\mathbf{z}|\mathcal{G})\|p(\mathbf{z})]. \quad (5)$$

Here $\hat{\mathcal{G}} = D(\mathbf{z})$, in which D denotes the decoder parameterized by HierVAE (Jin et al., 2020). $\text{KL}[q(\cdot)\|p(\cdot)]$ is the Kullback-Leibler (KL) divergence between $q(\cdot)$ and $p(\cdot)$. We follow Jin et al. (2020) and set the weight of KL loss $\alpha = 0.1$. Here, $p(\mathbf{z}) = \mathcal{N}(\mathbf{z}|\mathbf{0},\mathbf{I})$ is the isotropic multi-variate Gaussian prior, where \mathbf{I} is the identity matrix. We optimize this first expectation term concurrently through reparameterization trick (Kingma & Welling, 2013).

4.2. Multi-modal Molecule Latent Diffusion

We then introduce latent diffusion for conditional molecular graph generation, a method that leverages the aligned molecule-text latent space of encoder-decoder discussed above, enabling us preserve the crucial molecular properties and aligning the textual description of \mathcal{G} . Specifically, we learn a better probabilistic mapping from the text to the aligned molecule latent space, and thereby generate a higher-quality and more diverse molecules with more semantic consistency conforming to the conditional text inputs.

Specifically, the denoising network $\hat{\mathbf{z}}_\theta$ focuses on generating latent graph representation \mathbf{z} conditioned on the text representation \mathbf{c} from the text encoder E_t . The objective is:

$$\mathcal{L}_{\text{diff}} = \mathbb{E}_{t,\mathbf{x}_0,\epsilon} \left[\lambda_t \left\| \hat{\mathbf{z}}_\theta(\sqrt{\alpha_t}\mathbf{z} + \sqrt{1-\alpha_t}\epsilon, t, \mathbf{c}) - \mathbf{z} \right\|_2^2 \right], \quad (6)$$

where λ_t are time-dependent weights and we use MLPs for the network $\hat{\mathbf{z}}_\theta$. Specifically, we concatenate \mathbf{c} to graph latent representation \mathbf{z}_t for timestep t as the input of $\hat{\mathbf{z}}_\theta$. The denoising network is trained to denoise a noisy latent, $\mathbf{z}_t = \sqrt{\alpha_t}\mathbf{z} + \sqrt{1-\alpha_t}\epsilon$ to the clean \mathbf{z} . \mathbf{c} is the text representation from the fixed encoder E_t pretrained by Equation (4).

In addition, we improve sample quality through classifier-free guidance (Ho & Salimans, 2022), jointly training an unconditional network, $\hat{\mathbf{z}}_\theta(\mathbf{z}_t, t)$, and a conditional network, $\hat{\mathbf{z}}_\theta(\mathbf{z}_t, t, \mathbf{c})$. Conditioning information is randomly dropped with a probability of $p = 0.1$ during training. When conditioning information is dropped, we replace the embedded source text with a learnable embedding.

4.3. Training and Inference

Training. We now describe the training procedure for 3M-Diffusion. While the learning objectives for graph encoder-decoder and multi-modal latent diffusion have already been specified by Equations (5) and (6), it is unclear whether the two components should be trained sequentially

Previous research on latent diffusion models for image generation indicates that a two-stage training strategy often results in superior performance (Rombach et al., 2022). Hence, we adopt a similar two-stage strategy. Specifically, our first stage is to train the encoder-decoder using Equation (5), and the second stage is to train multi-modal molecule latent diffusion with the fixed encoder-decoder from stage one.

Inference. During inference, we use a weight w in computing the prediction as follows (Ho & Salimans, 2022):

$$\tilde{\mathbf{z}}_t = w\hat{\mathbf{z}}_\theta(\mathbf{z}_t, t, \mathbf{c}) + (1-w)\hat{\mathbf{z}}_\theta(\mathbf{z}_t, t), \quad (7)$$

where $\tilde{\mathbf{z}}_t$ represents the newly predicted results, incorporating both conditional and unconditional information. Setting $w = 1.0$ corresponds to the conditional diffusion model, while setting $w > 1.0$ enhances the impact of the conditioning information. A smaller value of w contributes to more diverse samples. The new sampling equation is:

$$\begin{aligned} \mathbf{z}_{t-1} = & \frac{\sqrt{\alpha_{t-1}}(1-\alpha_{t-1})}{1-\alpha_t} \tilde{\mathbf{z}}_t \\ & + \frac{\sqrt{\alpha_{t-1}}(1-\alpha_{t-1})}{1-\alpha_t} \mathbf{z}_t + \sigma(t-1, t)\epsilon, \end{aligned} \quad (8)$$

where the sampling chain is initialized from Gaussian prior $\mathbf{z}_T \sim p(\mathbf{z}_T) = \mathcal{N}(\mathbf{z}_T; \mathbf{0}, \mathbf{I})$. The detailed training and inference algorithms of 3M-diffusion are in Appendix B.

5. Experiment

5.1. Experimental Settings

Datasets. In our experiments, we use PubChem (Liu et al., 2023), ChEBI-20 (Edwards et al., 2021), PCDes (Zeng et al., 2022) and Momu (Su et al., 2022) datasets. Following the evaluation methodology adopted with datasets (ZINC250K (Irwin et al., 2012) and QM9 (Blum & Raymond, 2009; Rupp et al., 2012)) used in previous studies of automated generation of molecular structures, we limit our training, validation, and test data to molecules with fewer than 30 atoms. Statistics of datasets are shown in Table 3 and detailed descriptions are given in the Appendix C.1.

Evaluation. We evaluate the model’s performance on two tasks: text-guided and unconditional molecule generation. Following previous works on text-guided molecule generation, we compare our 3M-Diffusion the SOTA baselines (Edwards et al., 2022; Christofidellis et al., 2023). Text-guided molecule generation measures the model’s capacity to generate chemically valid, structurally diverse, novel molecules that match the textual description provided. Based on previous work (Chen et al., 2021; Fu et al., 2021; Wang et al., 2022), we adopt the following metrics for this task: *Similarity*, *Novelty*, *Diversity*, *Validity*. We call a predicted molecular graph, specifically one that is chemically valid (g'), *qualified* with the ground truth graph g if $f(g, g') > 0.5$, where f measures the MACCS (Durant et al., 2002) cosine

Table 1. Quantitative comparison of conditional generation on the ChEBI-20 and PubChem. 3M-Diffusion outperforms other SOTA methods in terms of novelty, diversity, and validity metrics by a large margin, while maintaining a good similarity metric.

# Metrics	PCDes				MoMu			
	Similarity (%)	Novelty (%)	Diversity (%)	Validity (%)	Similarity (%)	Novelty (%)	Diversity (%)	Validity (%)
MolT5-small	64.84	24.91	9.67	73.96	16.64	97.49	29.95	60.19
MolT5-base	71.71	25.85	10.50	81.92	19.76	97.78	29.98	68.84
MolT5-large	88.37	20.15	9.49	96.48	25.07	97.47	30.33	90.40
ChemT5-small	86.27	23.28	13.17	93.73	23.25	96.97	30.04	88.45
ChemT5-base	85.01	25.55	14.08	92.93	23.40	97.65	30.07	87.61
3M-Diffusion	81.57	63.66	32.39	100.0	24.62	98.16	37.65	100.0

Table 2. Quantitative comparison of conditional generation on the ChEBI-20 and PubChem. 3M-Diffusion outperforms other SOTA methods in terms of novelty, diversity, and validity metrics by a large margin, while maintaining a good similarity metric.

# Methods	ChEBI-20				PubChem			
	Similarity (%)	Novelty (%)	Diversity (%)	Validity (%)	Similarity (%)	Novelty (%)	Diversity (%)	Validity (%)
MolT5-small	73.32	31.43	17.22	78.27	68.36	20.63	9.32	78.86
MolT5-base	80.75	32.83	17.66	84.63	73.85	21.86	9.89	79.88
MolT5-large	96.88	12.92	11.20	98.06	91.57	20.85	9.84	95.18
ChemT5-small	96.22	13.94	13.50	96.74	89.32	20.89	13.10	93.47
ChemT5-base	95.48	15.12	13.91	97.15	89.42	22.40	13.98	92.43
3M-Diffusion	87.09	55.36	34.03	100	87.05	64.41	33.44	100

Table 3. Statistics of all datasets.

Dataset	#Training	#Validation	#Test
ChEBI-20	15,409	1,971	1,965
PubChem	6,912	571	1,162
PCDes	7,474	1,051	2,136
MoMu	7,474	1,051	4,554

similarity between the two. If the $f(g, g')$ similarity between g' and g is smaller than a threshold (0.8 in this paper), we call this predicted molecule g *novel*. Specifically, (i) *Similarity*: the percentage of qualified molecules out of 20K molecules; (ii) *Novelty*: the percentage of novel molecules out of all qualified molecules; (iii) *Diversity*: the average pairwise distance $1 - f(\cdot, \cdot)$ between all qualified molecules. (iv) *Validity*: the percentage of generated molecules that are chemically valid out of all molecules.

We report the results for unconditional molecule generation tasks using the GuacaMol benchmarks (Brown et al., 2019) to assess the model’s capability to learn molecular data distribution and generate realistic, diverse molecules. Specifically, *Uniqueness* gauges the ratio of unique molecules among the generated ones. *Novelty* measures the models’ capacity to generate molecules not present in the training set. *KL Divergence* assesses the proximity between the distributions of various physicochemical properties in the training set and the generated molecules. *Fréchet ChemNet Distance* (FCD) computes the proximity of two sets of molecules based on their hidden representations in ChemNet (Preuer et al., 2018). Each metric is normalized to a range of 0 to 1, with a higher value indicating better performance.

Baselines. For text guided molecule generation, we com-

pare 3M-Diffusion with the following baselines: MolT5 (Edwards et al., 2022) and ChemT5 (Christofidellis et al., 2023). We consider three representative baselines for unconditional molecule generation based on Variational Autoencoder, including BwR (Diamant et al., 2023), HierVAE (Jin et al., 2020) and PS-VAE (Kong et al., 2022). The descriptions and details of the baselines are given in Appendix C.1.

Setup. We randomly initialize the model parameters and use the Adam optimizer to train the model. HierVAE is used as our variational autoencoder for all of the following experiments. For baselines of unconditional generation that did not report results in these datasets, we reproduce the results using the official code of the authors. To ensure a fair comparison across all methods for unconditional generation, we select the best hyperparameter configuration solely based on the loss on the training set. We evaluate the performance of baselines for text-guided molecule generation using the released pre-trained parameters.

5.2. Text-guided Molecule Generation

Table 1 and 2 report *Similarity*, *Novelty*, *Diversity*, and *Validity* for text-guided molecule generation on four datasets. All of these metrics are computed as averages, with each metric being calculated based on 5 samples generated from each textual description. Our model demonstrates competitive results in *Similarity* and notably higher values in the *Diversity* and *Novelty*. Specifically, 3M-Diffusion achieves 146.27% (Novelty of PCDes), 130.04% (Diversity of PCDes) relative improvement over the second-best method with maintaining semantics in the textual prompt. This suggests that transformer-based models, pre-trained on a large dataset,

Table 4. Quantitative comparison of unconditional generation. Results of Uniq, KL Div and FCD on ChEBI-20 and PubChem, which refer to Uniqueness, KL Divergence and Fréchet ChemNet Distance, respectively. A higher number indicates a better generation quality.

# Methods	ChEBI-20					PubChem				
	Uniq (%)	Novelty (%)	KL Div (%)	FCD (%)	Validity (%)	Uniq (%)	Novelty (%)	KL Div (%)	FCD (%)	Validity (%)
BwR	22.09	21.97	50.59	0.26	22.66	82.35	82.34	45.53	0.11	87.73
HierVAE	82.17	72.83	93.39	64.32	100.0	75.33	72.44	89.05	50.04	100.0
PS-VAE	76.09	74.55	83.16	32.44	100.0	66.97	66.52	83.41	14.41	100.0
3M-Diffusion	83.04	70.80	96.29	77.83	100.0	85.42	81.20	92.67	58.27	100.0

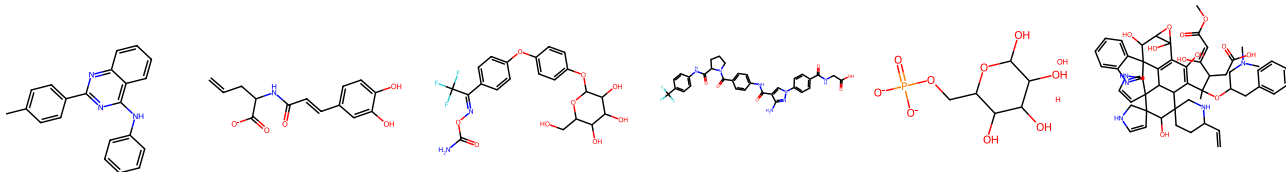


Figure 3. Molecules generated unconditionally by 3M-diffusion from the prior distribution $\mathcal{N}(\mathbf{0}, \mathbf{I})$.

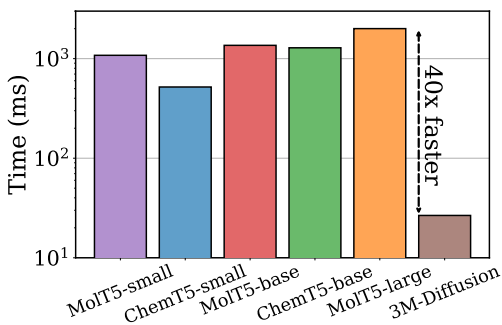


Figure 4. The average inference time comparison of molecule conditional generation on ChEBI-20 dataset.

excel in predicting molecules based on textual descriptions. However, our model can generate a diverse and novel collection of molecular graphs that match the textual descriptions provided as input. Also, as Figure 4 shows, our model can generate molecules faster than transformer-based methods.

5.3. Unconditional Molecule Generation

Table 4 shows the results of unconditional molecule generation on PubChem and ChEBI-20. 3M-Diffusion consistently outperforms or achieves competitive results across all four metrics on both datasets, indicating its ability to generate realistic molecules while avoiding overfitting the training data. Furthermore, 3M-Diffusion consistently outperforms HierVAE when both methods use the same decoder. This underscores the clear advantage of 3M-Diffusion in generating a diverse and novel assortment of molecular graphs. As shown in Figure 3, our sampled molecules present rich variety and structural complexity. We have included more sampled molecules from the prior distribution in Appendix D.4.

5.4. Ablation Study

We conduct ablation studies to assess the impact of different model designs, including joint training of the diffusion model and Variational Autoencoder (denoted as "Without

two stage training") and training the model without aligning the representation space of graphs and text using \mathcal{L}_{con} in Equation (4) (denoted as "Without representation alignment"). Additionally, we perform experiments without using either of these configurations, labeled as "Without two stage training & Without representation alignment" in Table 5. Initially, training the aligned encoder-decoder alongside Multi-modal Molecule Latent Diffusion jointly yielded comparable or superior performance in terms of diversity and novelty. However, there was a noticeable deficiency in its ability to learn align its representation of molecular graphs with that of their textual descriptions. Training 3M-Diffusion without the aligned encoder-decoder results in substantial drop in performance relative to 3M-Diffusion. This result underscores the importance of aligning the representation of textual descriptions of molecules with that of molecular graphs. Without using both design, Similarity suffers a substantial decline to 10.24, rendering it unsuitable for real-world applications. The full 3M-Diffusion model (last row) achieves the best performance with respect to all of the metrics. This confirms the suitability of the two-step training approach for generating diverse, novel set of molecules based on their textual descriptions.

5.5. Qualitative Analysis and Case Study

Property Conditional Molecule Generation. In traditional molecule generation models, the generation process is often conditioned on specific molecular properties such as logP (Kusner et al., 2017) and QED. logP assesses a molecule’s solubility, while QED evaluates its drug likeness (Bickerton et al., 2012). Previous methods have explored ways to optimize their models further in order to generate molecules with desired properties. However, in the case of our model, a different approach is taken. Our model utilizes designed prompts to realize the conditional molecule generation process, as illustrated in Figure 2 for assessing molecule solubility. In particular, we generated 10 samples for each prompt and subsequently select the top 5 samples

Table 5. Results of ablation study with different model designs of 3M-diffusion for the Pubchem dataset.

# Methods	Similarity (%)	Novelty (%)	Diversity (%)	Validity (%)
(i) Without two-stage training	77.74	67.03	31.05	100.0
(ii) Without representation alignment	86.21	62.81	32.78	100.0
(iii) Without two-stage training & representation alignment	10.24	77.89	27.86	100.0
3M-Diffusion	87.05	64.41	33.44	100.0



Figure 5. Molecules generated conditionally on input text by 3M-Diffusion on the ChEBI-20 dataset.

based on the desired property values. For MolT5-large, we adjust the temperature of the transformer in an attempt to encourage diversity while ensuring that invalid samples are controlled during the sampling process. We applied the same methodology used in our previous experiments to maintain consistency across the comparative analysis, as shown in Figure 2. Compared with the MolT5-large model, we find that 3M-Diffusion excels in generating a diverse range of molecules while achieving improved desired properties, as evidenced by higher logP values Figure 2. This underscores our model’s capacity to produce molecules that are not only novel and diverse but also match the textual description provided. This unique approach distinguishes 3M-Diffusion from prior methods for molecular generation, presenting a fresh and promising perspective on molecular design. For additional experimental details and insights regarding prompts related to solubility and drug likeness, please refer to the Appendix D.1.

Qualitative Comparison. In Figure 2, we introduce more specific prompts related to molecular categories, such as “The molecule is a member of the class of flavones.” These prompts bias the model, in favor of generating useful drug candidates. Specifically, we choose a reference molecule from the training dataset that matches the given textual prompt. Subsequently, we generate ten additional molecules and select the top five molecules that exhibit the highest structural similarity (calculated by Rascal algorithm (Raymond et al., 2002)) to the reference molecule. These selected molecules are shown in Figure 2. Comparison of our model with MolT5-large shows that our model generates more diverse molecules that exhibit a higher degree of structural similarity to the reference molecule. Simultaneously, it also produces novel molecular graphs. We also include more prompt examples in Appendix D.2.

Case Study. In Figure 5, we choose a set of examples from the ChEBI-20 dataset to visually illustrate the structural similarity between the molecules generated by 3M-Diffusion

and the ground truth molecules corresponding to the given text descriptions. Specifically, we show the largest substructure that appears in generated and ground truth molecules by RDKit. 3M-Diffusion demonstrates the capability to generate molecules that share a common substructure, as illustrated in Figure 5. Simultaneously, it has the flexibility to explore novel components or structures, thereby achieving a balance between generating similar structures and introducing novel molecules. This observation further confirms the ability of our model in generating a diverse collection of novel molecular structures that match the textual description provided. We show more results in Appendix D.3.

6. Conclusion

Generating molecules with desired properties is a critical task with broad applications in drug discovery and materials design. These applications call for methods that generate diverse, and ideally novel, molecules with the desired properties. We have introduced 3M-Diffusion, a novel multi-modal molecular graph generation method, to address this challenge. 3M-Diffusion first encodes molecular graphs into a graph latent space aligned with text descriptions. It then reconstructs the molecular graph and atomic attributes based on the given text descriptions using the molecule decoder. 3M-Diffusion learns a probabilistic mapping from the text space to the latent molecular graph space using the latent diffusion model. The results of our extensive experiments demonstrate that 3M-Diffusion can generate high-quality, novel and diverse molecular graphs that semantically match the textual description provided. Ablation studies underscore the importance of aligning the latent representation of texts with that of molecular graphs to the performance of 3M-Diffusion. Work in progress is aimed at text-guided molecular graph generation tasks, e.g., text-guided generation of biological macromolecules, new drugs and new materials, and experimental validation of the resulting graphs through their synthesis and characterization in the lab.

References

- Beltagy, I., Lo, K., and Cohan, A. Scibert: A pre-trained language model for scientific text. *arXiv preprint arXiv:1903.10676*, 2019.
- Bickerton, G. R., Paolini, G. V., Besnard, J., Muresan, S., and Hopkins, A. L. Quantifying the chemical beauty of drugs. *Nature chemistry*, 4(2):90–98, 2012.
- Bjerrum, E. J. and Threlfall, R. Molecular generation with recurrent neural networks (rnns). *arXiv preprint arXiv:1705.04612*, 2017.
- Blum, L. C. and Reymond, J.-L. 970 million druglike small molecules for virtual screening in the chemical universe database gdb-13. *Journal of the American Chemical Society*, 131(25):8732–8733, 2009.
- Brown, N., Fiscato, M., Segler, M. H., and Vaucher, A. C. Guacamol: benchmarking models for de novo molecular design. *Journal of chemical information and modeling*, 59(3):1096–1108, 2019.
- Chen, B., Wang, T., Li, C., Dai, H., and Song, L. Molecule optimization by explainable evolution. In *International conference on learning representation (ICLR)*, 2021.
- Christofidellis, D., Giannone, G., Born, J., Winther, O., Laino, T., and Manica, M. Unifying molecular and textual representations via multi-task language modelling. *arXiv preprint arXiv:2301.12586*, 2023.
- Diamant, N. L., Tseng, A. M., Chuang, K. V., Biancalani, T., and Scalia, G. Improving graph generation by restricting graph bandwidth. In *International Conference on Machine Learning*, pp. 7939–7959. PMLR, 2023.
- Du, Y., Fu, T., Sun, J., and Liu, S. Molgensurvey: A systematic survey in machine learning models for molecule design. *arXiv preprint arXiv:2203.14500*, 2022.
- Durant, J. L., Leland, B. A., Henry, D. R., and Nourse, J. G. Reoptimization of mdl keys for use in drug discovery. *Journal of chemical information and computer sciences*, 42(6):1273–1280, 2002.
- Edwards, C., Zhai, C., and Ji, H. Text2mol: Cross-modal molecule retrieval with natural language queries. In *Proceedings of the 2021 Conference on Empirical Methods in Natural Language Processing*, pp. 595–607, 2021.
- Edwards, C., Lai, T., Ros, K., Honke, G., Cho, K., and Ji, H. Translation between molecules and natural language. *arXiv preprint arXiv:2204.11817*, 2022.
- Fang, Y., Liang, X., Zhang, N., Liu, K., Huang, R., Chen, Z., Fan, X., and Chen, H. Mol-instructions: A large-scale biomolecular instruction dataset for large language models. *arXiv preprint arXiv:2306.08018*, 2023a.
- Fang, Y., Zhang, N., Chen, Z., Fan, X., and Chen, H. Molecular language model as multi-task generator. *arXiv preprint arXiv:2301.11259*, 2023b.
- Flam-Shepherd, D., Zhu, K., and Aspuru-Guzik, A. Language models can learn complex molecular distributions. *Nature Communications*, 13(1):3293, 2022.
- Fu, T., Gao, W., Xiao, C., Yasonik, J., Coley, C. W., and Sun, J. Differentiable scaffolding tree for molecular optimization. *arXiv preprint arXiv:2109.10469*, 2021.
- Gómez-Bombarelli, R., Wei, J. N., Duvenaud, D., Hernández-Lobato, J. M., Sánchez-Lengeling, B., Sheberla, D., Aguilera-Iparraguirre, J., Hirzel, T. D., Adams, R. P., and Aspuru-Guzik, A. Automatic chemical design using a data-driven continuous representation of molecules. *ACS central science*, 4(2):268–276, 2018.
- Goyal, N., Jain, H. V., and Ranu, S. Graphgen: A scalable approach to domain-agnostic labeled graph generation. In *Proceedings of The Web Conference 2020*, pp. 1253–1263, 2020.
- Grisoni, F. Chemical language models for de novo drug design: Challenges and opportunities. *Current Opinion in Structural Biology*, 79:102527, 2023.
- Grover, A., Zweig, A., and Ermon, S. Graphite: Iterative generative modeling of graphs. In *International conference on machine learning*, pp. 2434–2444. PMLR, 2019.
- Guarino, M., Shah, A., and Rivas, P. Dipol-gan: Generating molecular graphs adversarially with relational differentiable pooling. *Under review*, 2017.
- Hajduk, P. J. and Greer, J. A decade of fragment-based drug design: strategic advances and lessons learned. *Nature reviews Drug discovery*, 6(3):211–219, 2007.
- Hastings, J., Owen, G., Dekker, A., Ennis, M., Kale, N., Muthukrishnan, V., Turner, S., Swainston, N., Mendes, P., and Steinbeck, C. ChEBI in 2016: Improved services and an expanding collection of metabolites. *Nucleic acids research*, 44(D1):D1214–D1219, 2016.
- Ho, J. and Salimans, T. Classifier-free diffusion guidance. *arXiv preprint arXiv:2207.12598*, 2022.
- Ho, J., Jain, A., and Abbeel, P. Denoising diffusion probabilistic models. *Advances in neural information processing systems*, 33:6840–6851, 2020.
- Hu, W., Liu, B., Gomes, J., Zitnik, M., Liang, P., Pande, V., and Leskovec, J. Strategies for pre-training graph neural networks. *arXiv preprint arXiv:1905.12265*, 2019.

- Irwin, J. J., Sterling, T., Mysinger, M. M., Bolstad, E. S., and Coleman, R. G. Zinc: a free tool to discover chemistry for biology. *Journal of chemical information and modeling*, 52(7):1757–1768, 2012.
- Jin, W., Barzilay, R., and Jaakkola, T. Junction tree variational autoencoder for molecular graph generation. In *International conference on machine learning*, pp. 2323–2332. PMLR, 2018.
- Jin, W., Barzilay, R., and Jaakkola, T. Hierarchical generation of molecular graphs using structural motifs. In *International conference on machine learning*, pp. 4839–4848. PMLR, 2020.
- Jo, J., Lee, S., and Hwang, S. J. Score-based generative modeling of graphs via the system of stochastic differential equations. In *International Conference on Machine Learning*, pp. 10362–10383. PMLR, 2022.
- Kim, S., Thiessen, P. A., Bolton, E. E., Chen, J., Fu, G., Gindulyte, A., Han, L., He, J., He, S., Shoemaker, B. A., et al. Pubchem substance and compound databases. *Nucleic acids research*, 44(D1):D1202–D1213, 2016.
- Kingma, D. P. and Ba, J. Adam: A method for stochastic optimization. *arXiv preprint arXiv:1412.6980*, 2014.
- Kingma, D. P. and Welling, M. Auto-encoding variational bayes. *arXiv preprint arXiv:1312.6114*, 2013.
- Kong, X., Huang, W., Tan, Z., and Liu, Y. Molecule generation by principal subgraph mining and assembling. *Advances in Neural Information Processing Systems*, 35: 2550–2563, 2022.
- Krenn, M., Ai, Q., Barthel, S., Carson, N., Frei, A., Frey, N. C., Friederich, P., Gaudin, T., Gayle, A. A., Jablonka, K. M., et al. Selfies and the future of molecular string representations. *Patterns*, 3(10), 2022.
- Kusner, M. J., Paige, B., and Hernández-Lobato, J. M. Grammar variational autoencoder. In *International conference on machine learning*, pp. 1945–1954. PMLR, 2017.
- Li, Y., Vinyals, O., Dyer, C., Pascanu, R., and Battaglia, P. Learning deep generative models of graphs. *arXiv preprint arXiv:1803.03324*, 2018.
- Liu, Q., Allamanis, M., Brockschmidt, M., and Gaunt, A. Constrained graph variational autoencoders for molecule design. *Advances in neural information processing systems*, 31, 2018.
- Liu, Z., Li, S., Luo, Y., Fei, H., Cao, Y., Kawaguchi, K., Wang, X., and Chua, T.-S. Molca: Molecular graph-language modeling with cross-modal projector and uni-modal adapter. *arXiv preprint arXiv:2310.12798*, 2023.
- Lo, K., Wang, L. L., Neumann, M., Kinney, R., and Weld, D. S. S2orc: The semantic scholar open research corpus. *arXiv preprint arXiv:1911.02782*, 2019.
- Luo, Y., Yan, K., and Ji, S. Graphdf: A discrete flow model for molecular graph generation. In *International Conference on Machine Learning*, pp. 7192–7203. PMLR, 2021.
- Madhawa, K., Ishiguro, K., Nakago, K., and Abe, M. Graph-nvp: An invertible flow model for generating molecular graphs. *arXiv preprint arXiv:1905.11600*, 2019.
- Mandal, S., Mandal, S. K., et al. Rational drug design. *European journal of pharmacology*, pp. 90–100, 2009.
- Maziarka, Ł., Pocha, A., Kaczmarczyk, J., Rataj, K., Danel, T., and Warchoń, M. Mol-cyclegan: a generative model for molecular optimization. *Journal of Cheminformatics*, 12(1):1–18, 2020.
- Nichol, A. Q. and Dhariwal, P. Improved denoising diffusion probabilistic models. In *International Conference on Machine Learning*, pp. 8162–8171. PMLR, 2021.
- Niu, C., Song, Y., Song, J., Zhao, S., Grover, A., and Ermon, S. Permutation invariant graph generation via score-based generative modeling. In *International Conference on Artificial Intelligence and Statistics*, pp. 4474–4484. PMLR, 2020.
- OpenAI, R. Gpt-4 technical report. arxiv 2303.08774. *View in Article*, 2:13, 2023.
- Popova, M., Shvets, M., Oliva, J., and Isayev, O. Molecular-rnn: Generating realistic molecular graphs with optimized properties. *arXiv preprint arXiv:1905.13372*, 2019.
- Preuer, K., Renz, P., Unterthiner, T., Hochreiter, S., and Klambauer, G. Fréchet chemnet distance: a metric for generative models for molecules in drug discovery. *Journal of chemical information and modeling*, 58(9):1736–1741, 2018.
- Pyzer-Knapp, E. O., Suh, C., Gómez-Bombarelli, R., Aguilera-Iparraguirre, J., and Aspuru-Guzik, A. What is high-throughput virtual screening? a perspective from organic materials discovery. *Annual Review of Materials Research*, 45:195–216, 2015.
- Radford, A., Kim, J. W., Hallacy, C., Ramesh, A., Goh, G., Agarwal, S., Sastry, G., Askell, A., Mishkin, P., Clark, J., et al. Learning transferable visual models from natural language supervision. In *International conference on machine learning*, pp. 8748–8763. PMLR, 2021.
- Raffel, C., Shazeer, N., Roberts, A., Lee, K., Narang, S., Matena, M., Zhou, Y., Li, W., and Liu, P. J. Exploring

- the limits of transfer learning with a unified text-to-text transformer. *The Journal of Machine Learning Research*, 21(1):5485–5551, 2020.
- Raymond, J. W., Gardiner, E. J., and Willett, P. Rascal: Calculation of graph similarity using maximum common edge subgraphs. *The Computer Journal*, 45(6):631–644, 2002.
- Rombach, R., Blattmann, A., Lorenz, D., Esser, P., and Ommer, B. High-resolution image synthesis with latent diffusion models. In *Proceedings of the IEEE/CVF conference on computer vision and pattern recognition*, pp. 10684–10695, 2022.
- Rupp, M., Tkatchenko, A., Müller, K.-R., and Von Lilienfeld, O. A. Fast and accurate modeling of molecular atomization energies with machine learning. *Physical review letters*, 108(5):058301, 2012.
- Schwaller, P., Laino, T., Gaudin, T., Bolgar, P., Hunter, C. A., Bekas, C., and Lee, A. A. Molecular transformer: a model for uncertainty-calibrated chemical reaction prediction. *ACS central science*, 5(9):1572–1583, 2019.
- Schwaller, P., Probst, D., Vaucher, A. C., Nair, V. H., Kreutter, D., Laino, T., and Reymond, J.-L. Mapping the space of chemical reactions using attention-based neural networks. *Nature machine intelligence*, 3(2):144–152, 2021.
- Seidl, P., Vall, A., Hochreiter, S., and Klambauer, G. Enhancing activity prediction models in drug discovery with the ability to understand human language. *arXiv preprint arXiv:2303.03363*, 2023.
- Song, J., Meng, C., and Ermon, S. Denoising diffusion implicit models. *arXiv preprint arXiv:2010.02502*, 2020.
- Su, B., Du, D., Yang, Z., Zhou, Y., Li, J., Rao, A., Sun, H., Lu, Z., and Wen, J.-R. A molecular multimodal foundation model associating molecule graphs with natural language. *arXiv preprint arXiv:2209.05481*, 2022.
- Toniato, A., Schwaller, P., Cardinale, A., Geluykens, J., and Laino, T. Unassisted noise reduction of chemical reaction datasets. *Nature Machine Intelligence*, pp. 485–494, 2021.
- Vaucher, A. C., Zipoli, F., Geluykens, J., Nair, V. H., Schwaller, P., and Laino, T. Automated extraction of chemical synthesis actions from experimental procedures. *Nature communications*, 11(1):3601, 2020.
- Vignac, C., Krawczuk, I., Siraudin, A., Wang, B., Cevher, V., and Frossard, P. Digress: Discrete denoising diffusion for graph generation. *arXiv preprint*, 2022.
- Wang, Z., Nie, W., Qiao, Z., Xiao, C., Baraniuk, R., and Anandkumar, A. Retrieval-based controllable molecule generation. *arXiv preprint arXiv:2208.11126*, 2022.
- Weininger, D. Smiles, a chemical language and information system. 1. introduction to methodology and encoding rules. *Journal of chemical information and computer sciences*, 28(1):31–36, 1988.
- Xiao, T. and Wang, D. A general offline reinforcement learning framework for interactive recommendation. In *Proceedings of the AAAI Conference on Artificial Intelligence*, volume 35, pp. 4512–4520, 2021.
- Xiao, T., Chen, Z., Wang, D., and Wang, S. Learning how to propagate messages in graph neural networks. In *Proceedings of the 27th ACM SIGKDD Conference on Knowledge Discovery & Data Mining*, pp. 1894–1903, 2021.
- Xiao, T., Cui, C., Zhu, H., and Honavar, V. Molbind: Multimodal alignment of language, molecules, and proteins. *arXiv preprint*, 2023.
- Xiao, T., Zhu, H., Chen, Z., and Wang, S. Simple and asymmetric graph contrastive learning without augmentations. *Advances in Neural Information Processing Systems*, 36, 2024.
- Yin, S., Fu, C., Zhao, S., Li, K., Sun, X., Xu, T., and Chen, E. A survey on multimodal large language models. *arXiv preprint arXiv:2306.13549*, 2023.
- You, J., Liu, B., Ying, Z., Pande, V., and Leskovec, J. Graph convolutional policy network for goal-directed molecular graph generation. *Advances in neural information processing systems*, 31, 2018.
- Zang, C. and Wang, F. Moflow: an invertible flow model for generating molecular graphs. In *Proceedings of the 26th ACM SIGKDD international conference on knowledge discovery & data mining*, pp. 617–626, 2020.
- Zeng, Z., Yao, Y., Liu, Z., and Sun, M. A deep-learning system bridging molecule structure and biomedical text with comprehension comparable to human professionals. *Nature communications*, 13(1):862, 2022.
- Zhao, H., Liu, S., Ma, C., Xu, H., Fu, J., Deng, Z.-H., Kong, L., and Liu, Q. Gimlet: A unified graph-text model for instruction-based molecule zero-shot learning. *bioRxiv*, pp. 2023–05, 2023a.
- Zhao, Z., Liu, W., Chen, X., Zeng, X., Wang, R., Cheng, P., Fu, B., Chen, T., Yu, G., and Gao, S. Michelangelo: Conditional 3d shape generation based on shape-image-text aligned latent representation. *arXiv preprint arXiv:2306.17115*, 2023b.

Impact Statements

This paper advances machine learning approaches to text-guided generation of molecular graphs, with potential application in drug design and material discovery. If the resulting molecular graphs can be synthesized and experimentally characterized in the lab, the methods could be used to address societal needs for new drugs for combating diseases and for new materials for wideranging applications.

A. Diffusion Models

We present a formal description of diffusion (Ho et al., 2020; Song et al., 2020). Diffusion models are latent variable models that represent the data \mathbf{z}_0 as Markov chains $\mathbf{z}_T \cdots \mathbf{z}_0$, where intermediate variables share the same dimension. DMs involve a forward diffusion process $q(\mathbf{z}_{1:T} | \mathbf{z}_0) = \prod_{t=1}^T q(\mathbf{z}_t | \mathbf{z}_{t-1})$ and a reverse process $p_\theta(\mathbf{z}_{0:T}) = p(\mathbf{z}_T) \prod_{t=1}^T p_\theta(\mathbf{z}_{t-1} | \mathbf{z}_t)$. The forward process starting from \mathbf{z}_0 can be written as:

$$q(\mathbf{z}_t | \mathbf{x}_0) := \int q(\mathbf{z}_{1:t} | \mathbf{x}_0) d\mathbf{z}_{1:(t-1)} = \mathcal{N}(\mathbf{z}_t; \sqrt{\alpha_t} \mathbf{x}_0, (1 - \alpha_t) \mathbf{I}), \quad (9)$$

where the hyperparameter $\alpha_{1:T}$ determines the magnitude of noise added at each timestep t . The values of $\alpha_{1:T}$ are selected to ensure that samples \mathbf{z}_T converge to standard Gaussians, i.e., $q(\mathbf{z}_T) \approx \mathcal{N}(0, \mathbf{I})$. This forward process q is usually predefined without trainable parameters.

The generation process of DMs is defined as learning a parameterized reverse denoising process, which incrementally denoises the noisy variables $\mathbf{z}_{T:1}$ to approximate clean data x_0 in the target data distribution:

$$p_\theta(\mathbf{z}_{t-1} | \mathbf{z}_t) = \mathcal{N}(\mathbf{z}_{t-1}; \boldsymbol{\mu}_\theta(\mathbf{z}_t, t-1, t), \sigma^2(t-1, t) \mathbf{I}), \quad (10)$$

where the initial distribution $p(\mathbf{z}_T)$ is defined as $\mathcal{N}(0, \mathbf{I})$. The means $\boldsymbol{\mu}_\theta$ typically are neural networks such as U-Nets for images or Transformers for text, and the variances $\sigma^2(t-1, t)$ typically are also predefined. As latent variable models, the forward process $q(\mathbf{z}_{1:T} | \mathbf{z}_0)$ can be seen as a fixed posterior. The reverse process $p_\theta(\mathbf{z}_{0:T})$ is trained to maximize the variational lower bound of the likelihood of the data:

$$\mathcal{L}_{\text{vlb}} = \mathbb{E}_{q(\mathbf{z}_{1:T} | \mathbf{z}_0)} \left[\log \frac{q(\mathbf{z}_T | \mathbf{z}_0)}{p_\theta(\mathbf{z}_T)} + \sum_{t=2}^T \log \frac{q(\mathbf{z}_{t-1} | \mathbf{z}_0, \mathbf{z}_t)}{p_\theta(\mathbf{z}_{t-1} | \mathbf{z}_t)} - \log p_\theta(\mathbf{z}_0 | \mathbf{z}_1) \right] \quad (11)$$

To ensure training stability, a simple surrogate objective up to irrelevant constant terms is introduced (Song et al., 2020; Ho et al., 2020; Nichol & Dhariwal, 2021):

$$\mathcal{L}_{\text{diff}} = \mathbb{E}_{t, \mathbf{z}_0, \epsilon} \left[\lambda_t \|\hat{\mathbf{z}}_\theta(\sqrt{\alpha_t} \mathbf{z}_0 + \sqrt{1 - \alpha_t} \epsilon, t) - \mathbf{z}_0\|_2^2 \right], \quad (12)$$

where \mathbf{z}_t is used to denote $\sqrt{\alpha_t} \mathbf{z}_0 + \sqrt{1 - \alpha_t} \epsilon$ for simplicity. Intuitively, we train a neural network $\hat{\mathbf{z}}_\theta(\mathbf{z}_t, t)$ to approximate the original data given some noisy latent and the timestep through Equation (12), $\hat{\mathbf{z}}_\theta(\mathbf{z}_t, t) \approx \mathbf{z}$. With a trained denoising network, we define the mean and variance function in Equation (10) following the previous work (Ho et al., 2020) as:

$$\boldsymbol{\mu}_\theta(\mathbf{z}_t, t-1, t) = \frac{\sqrt{\alpha_{t-1}}(1 - \alpha_{t|t-1})}{1 - \alpha_t} \hat{\mathbf{z}}_\theta(\mathbf{z}_t, t) + \frac{\sqrt{\alpha_{t|t-1}}(1 - \alpha_{t-1})}{1 - \alpha_t} \mathbf{z}_t, \sigma^2(t-1, t) = \frac{(1 - \alpha_{t-1})(1 - \alpha_{t|t-1})}{1 - \alpha_t}, \quad (13)$$

where λ_t is the time-dependent weight and $\alpha_{t|t-1} = \alpha_t / \alpha_{t-1}$. For generation, we employ the standard DDPM sampler, also referred to as the ancestral sampler (Ho et al., 2020). The process involves sampling initial noise $\mathbf{z}_T \sim \mathcal{N}(\mathbf{0}, \mathbf{I})$ and iteratively applying the update rule:

$$\mathbf{z}_{t-1} = \frac{\sqrt{\alpha_{t-1}}(1 - \alpha_{t|t-1})}{1 - \alpha_t} \hat{\mathbf{z}}_\theta(\mathbf{z}_t, t) + \frac{\sqrt{\alpha_{t|t-1}}(1 - \alpha_{t-1})}{1 - \alpha_t} \mathbf{z}_t + \sigma(t-1, t) \epsilon, \quad (14)$$

where $\epsilon \sim \mathcal{N}(\mathbf{0}, \mathbf{I})$. We use $T = 50$ for the sampling timesteps.

Algorithm 1 Training Algorithm of 3M-Diffusion

```

1: Input: Pairs of Molecule Graph data  $\mathcal{G} = (\mathcal{V}, \mathcal{E})$  and Textual Description  $\mathcal{T}$ 
2: Initial: Graph Encoder network  $E_g$ , Text Encoder network  $E_t$  and Decoder network  $D$ , denoising network  $\hat{z}_\theta$ 
3: Pretraining Stage: Aligned Text and Graph Encoder Training
4: while  $E_g$  and  $E_t$  have not converged do
5:    $\mathcal{L}_{\text{con}} = -\frac{1}{|\mathcal{B}|} \sum_{(\mathcal{G}_i, \mathcal{T}_i) \in \mathcal{B}} \log \frac{\exp(\cos(\mathbf{z}_i, \mathbf{c}_i)/\tau)}{\sum_{j=1}^{|\mathcal{B}|} \exp(\cos(\mathbf{z}_i, \mathbf{c}_j)/\tau)}$ 
6:    $E_g, E_t \leftarrow \text{optimizer}(\mathcal{L}_{\text{con}})$ 
7: end while
8: First Stage: Autoencoder Training
9: Initialize  $E_g$  from Pretraining Stage
10: while  $E_g$  and  $D$  have not converged do
11:    $\mathbf{z} \leftarrow E_g(\mathcal{G})$ 
12:    $\mathcal{G} \leftarrow D(\mathbf{z})$  ▶ Decoding
13:    $\mathcal{L}_{\text{elbo}} = -\mathbb{E}_{q(\mathbf{z}|\mathbf{A}, \mathbf{x})} [p(\mathcal{G} | \hat{\mathcal{G}})] + \alpha \text{KL}[q(\mathbf{z} | \mathcal{G}) \| p(\mathbf{z})]$ 
14:    $E_g, D \leftarrow \text{optimizer}(\mathcal{L}_{\text{elbo}})$ 
15: end while
16: Second Stage: Multi-modal Molecule Latent Diffusion Training
17: Fix Graph Encoder  $E_g$  from Stage 1 and Text Encoder  $E_t$  from Pretraining Stage
18: while  $\mathbf{z}_\theta$  have not converged do
19:    $\mathbf{z} \leftarrow E_g(\mathcal{G})$ 
20:    $t \sim \mathbf{U}(0, T), \epsilon \sim \mathcal{N}(\mathbf{0}, \mathbf{I})$ 
21:    $\mathcal{L}_{\text{diff}} = \mathbb{E}_{t, \mathbf{x}_0, \epsilon} \left[ \lambda_t \left\| \hat{\mathbf{z}}_\theta \left( \sqrt{\alpha_t} \mathbf{z}_0 + \sqrt{1 - \alpha_t} \epsilon, t \right) - \mathbf{z}_0 \right\|_2^2 \right]$ 
22:    $\theta \leftarrow \text{optimizer}(\mathcal{L}_{\text{diff}})$ 
23: end while
24: return  $E_g, D$ 

```

Algorithm 2 Sampling Algorithm of 3M-Diffusion

```

1: Input: decoder network  $D$ , denoising network  $\hat{z}_\theta$ 
2:  $\mathbf{z}_T \sim \mathcal{N}(\mathbf{0}, \mathbf{I})$ 
3: for  $t$  in  $T, T-1, \dots, 1$  do
4:    $\epsilon \sim \mathcal{N}(\mathbf{0}, \mathbf{I})$  ▶ Latent Denoising Loop
5:    $\tilde{\mathbf{z}}_t = w \hat{\mathbf{z}}_\theta(\mathbf{z}_t, t, \mathbf{c}) + (1-w) \hat{\mathbf{z}}_\theta(\mathbf{z}_t, t),$ 
6:    $\mathbf{z}_{t-1} = \frac{\sqrt{\alpha_{t-1}(1-\alpha_t|_{t-1})}}{1-\alpha_t} \tilde{\mathbf{z}}_t + \frac{\sqrt{\alpha_t|_{t-1}(1-\alpha_{t-1})}}{1-\alpha_t} \mathbf{z}_t + \sigma(t-1, t) \epsilon$ 
7: end for
8:  $\mathcal{G} \sim p(\mathcal{G}|\mathbf{z}_0)$  ▶ Decoding
9: return  $\mathbf{x}, \mathbf{h}$ 

```

B. Training and Sampling Algorithm

The complete training algorithm is depicted in Algorithm 1. Firstly, the process begins by training the graph and text encoders using contrastive learning. Following that, the Variational Autoencoder is trained to facilitate the reconstruction of molecule graphs. Lastly, the Multi-modal Molecule Latent Diffusion Model is employed to train the denoising network for the sampling process. This structured approach forms the core of our training procedure. Moreover, we present the sampling method of 3M-Diffusion in Algorithm 2.

C. Experimental Details

C.1. Datasets Details and Statistics

The statistics of datasets, including their the number of samples for training, validation and test sets are given in Table 3.

ChEBI-20 (Edwards et al., 2021): This dataset is generated by leveraging PubChem (Kim et al., 2016) and Chemical

Entities of Biological Interest (ChEBI) (Hastings et al., 2016). It compiles ChEBI annotations of compounds extracted from PubChem, comprising molecule-description pairs. To ensure less noise and more informative molecule descriptions, it includes samples with descriptions exceeding 20 words.

PubChem (Liu et al., 2023): This dataset comprises 324k molecule-text pairs gathered from the PubChem website. As the dataset contains numerous uninformative texts like "The molecule is a peptide," it curates a high-quality subset of 15k pairs with text longer than 19 words for downstream tasks. This refined subset is then randomly split into training, validation, and test sets. The remaining dataset, which is more noisy, is utilized for pretraining. To prevent data leakage, we exclude samples that appear in the testing set of other datasets from the pretraining dataset.

PCDes (Zeng et al., 2022): This dataset compiles molecule-text pairs sourced from PubChem (Kim et al., 2016), encompassing names, SMILES notations, and accompanying paragraphs providing property descriptions for each molecule.

MoMu (Su et al., 2022): This dataset comprises paired molecule graph-text data, with the textual information for each molecule extracted from the SCI paper dataset (Lo et al., 2019).

For all datasets, inspired by previous datasets (ZINC250K (Irwin et al., 2012) and QM9 (Blum & Reymond, 2009; Rupp et al., 2012)) on molecule generation, we preserve molecules with fewer than 30 atoms, creating new training, validation, and test sets from their original counterparts.

C.2. Baselines

We firstly introduce the baselines used for text-guided molecule generation in this section.

MolT5 (Edwards et al., 2022): MolT5 addresses the difficult problem of cross-domain generation by linking natural language and chemistry, tackling tasks such as text-conditional molecule generation and molecule captioning. It presents several T5-based LMs (Raffel et al., 2020) by training on the SMILES-to-text and text-to-SMILES translations.

ChemT5 (Christofidellis et al., 2023): ChemT5 introduces a versatile multi-task model for seamless translation between textual and chemical domains. This innovative approach leverages transfer learning in the chemical domain, with a particular emphasis on addressing cross-domain tasks that involve both chemistry and natural language.

Then, we will also include three baselines for unconditional generation to verify the effectiveness of our model.

BwR (Diamant et al., 2023): BwR aims to decrease the time/space complexity and output space of graph generative models, demonstrating notable performance improvements in generating high-quality outputs on biological and chemical datasets.

HierVAE (Jin et al., 2020): HierVAE employs a hierarchical encoder-decoder architecture to generate molecular graphs, leveraging structural motifs as fundamental building blocks.

PS-VAE (Kong et al., 2022): PS-VAE automatically identifies regularities within molecules, extracting them as principal subgraphs. Utilizing these extracted principal subgraphs, it proceeds to generate molecules in two distinct phases.

C.3. Setup and Hyper-parameter settings

We use official implementation publicly released by the authors of the baselines or implementation from Pytorch. Note that we use the decoder of HierVAE for our model. We run experiments on a machine with a NVIDIA A100 GPU with 80GB of GPU memory. In all experiments, we use the Adam optimizer (Kingma & Ba, 2014). In particular, for our 3M-diffusion, we set the dimension of latent representation as 24, the number of layers for the denosing networks (MLP) as 4, α as 0.1, T as 100 for training and 50 for sampling process and the probability $p = 0.8$ for text-guided molecule generation. For unconditional generation, we set T as 10 or 5 for the sampling process.

D. More Visualization Results

D.1. Property Conditional Molecule Generation

In this section, we provide more prompt examples and more experiment details for Property Conditional Molecule Generation. We generate 10 samples for each prompt and subsequently select the top 5 samples based on the desired property values, as shown in Figure 2, 6, 7 and 8. For instance, when using the prompt "This molecule is not like a drug," we select the top 5 molecules with the smallest QED values, as indicated. Conversely, for the prompt "This molecule is like a drug," we opt for

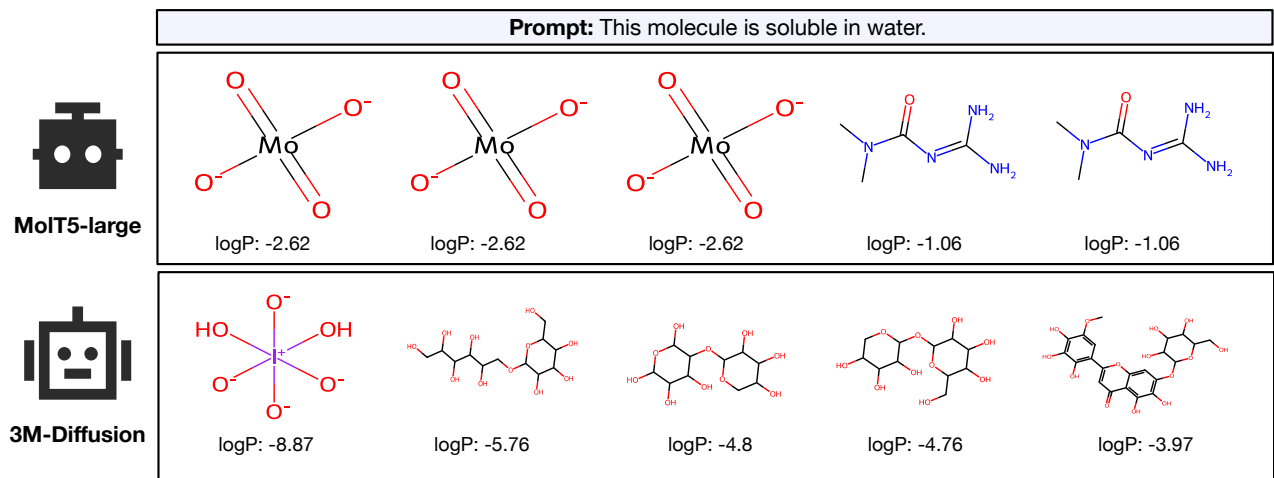


Figure 6. Qualitative comparisons to the MolT5-large in terms of generated molecules on CheBI-20. Compared with the SOTA method MolT5-large, our generated results are more diverse and novel with maintained semantics in textual prompt.

the top 5 molecules with the largest QED values. This same approach is applied to solubility, where we select molecules based on logP values. Specifically, we adjust temperature setting within the MolT5 transformer model to promote the generation of diverse molecules. We carefully selected an appropriate temperature threshold that struck a balance between diversity and maintaining the validity of the generated molecules. Moreover, when dealing with MolT5, it is worth noting that it may occasionally generate multiple unconnected molecules within a single SMILES representation. In such cases, we select the molecule among these unconnected ones that best aligns with the top desired attribute. From all figures, it becomes evident that our model excels in generating molecules with improved desired properties when compared to MolT5-large.

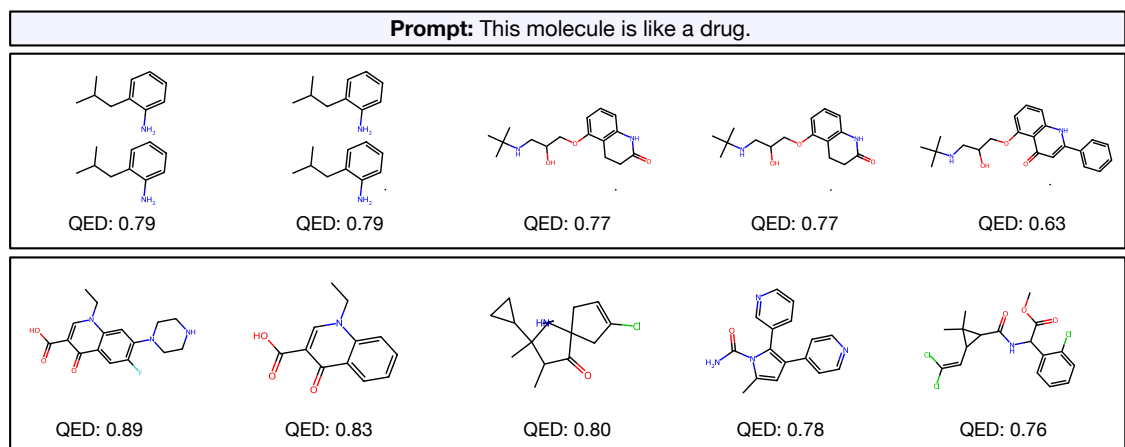


Figure 7. Qualitative comparisons to the MolT5-large in terms of generated molecules on CheBI-20. Compared with the SOTA method MolT5-large, our generated results are more diverse and novel with maintained semantics in textual prompt.

D.2. Qualitative Comparison

In this section, we introduce an additional prompt example: "The molecule is an anthocyanidin cation." This prompt is used to generate molecules belonging to specific categories. We have the same observation that our model excels in generating molecules that not only closely resemble the reference molecule but also encompass some diverse and novel structures.

D.3. Case Study

In this section, we choose 20 more examples from the ChEBI-20 dataset to visually illustrate the structural similarity between the molecules generated by 3M-Diffusion and the ground truth molecules corresponding to the given text descriptions. All results are shown in Figure 5. We also observe that our model is proficient at generating molecules that share significant

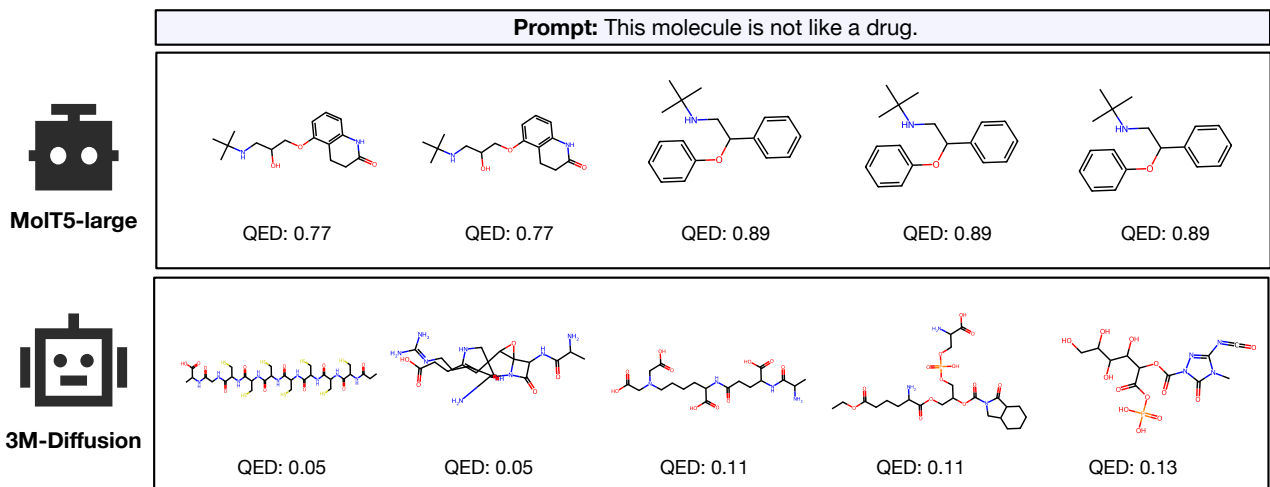


Figure 8. Qualitative comparisons to the MolT5-large in terms of generated molecules on CheBI-20. Compared with the SOTA method MolT5-large, our generated results are more diverse and novel with maintained semantics in textual prompt.

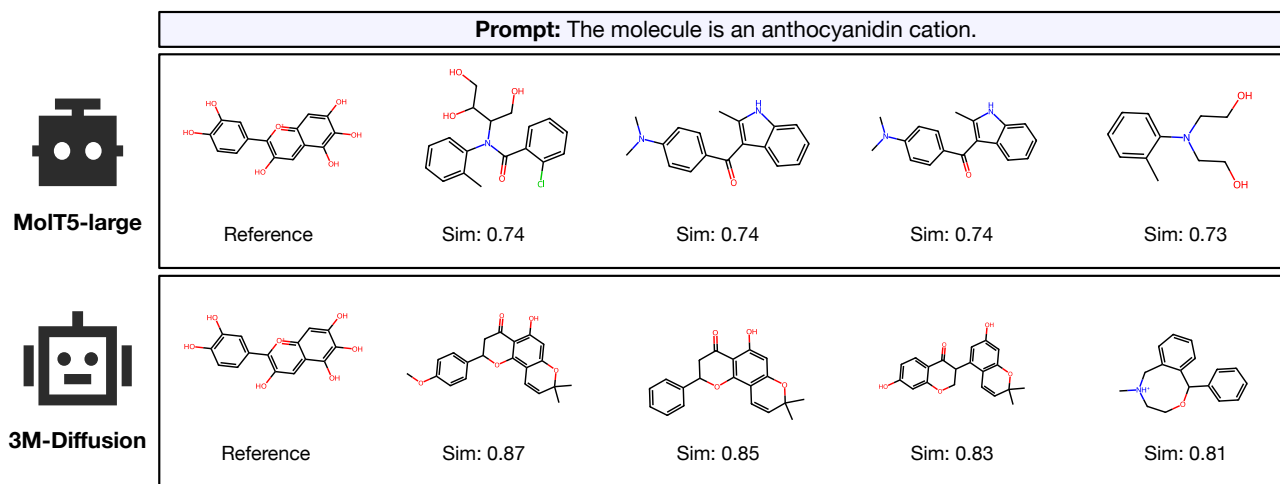


Figure 9. Qualitative comparisons to the MolT5-large in terms of generated molecules on CheBI-20. Compared with the SOTA method MolT5-large, our generated results are more diverse and novel with maintained semantics in textual prompt.

common structural elements, while simultaneously obtaining diverse and innovative molecular structures.

D.4. Unconditional Molecule Generation

We further present 50 molecules sampled from the prior distribution in Figure 11. As shown in Figure 11, our sampled molecules present rich variety and structural complexity. This demonstrates our model’s ability to generate diverse, novel, and realistic molecules.

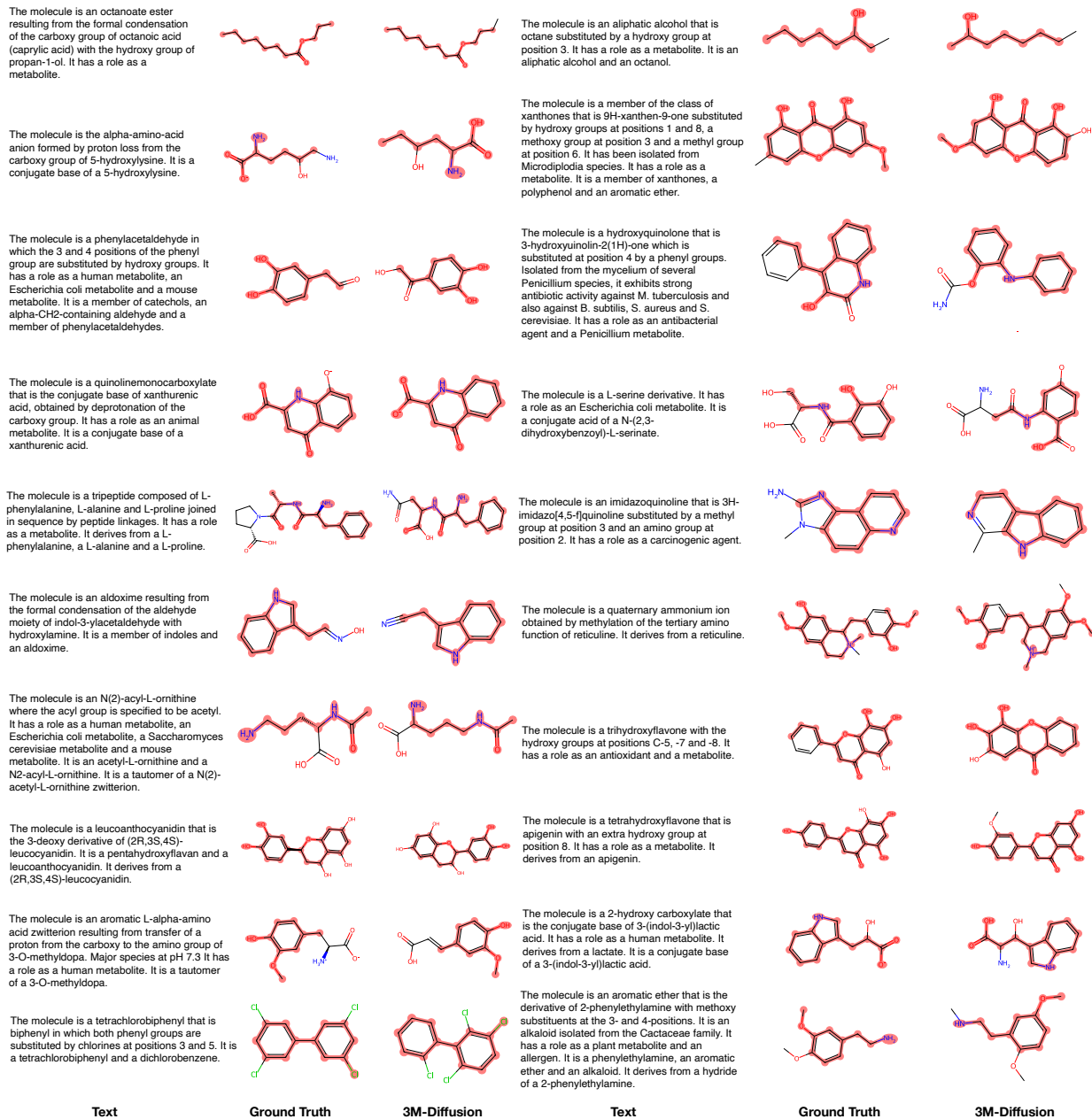


Figure 10. More molecules generated conditionally on input text by 3M-Diffusion on the ChEBI-20 dataset.

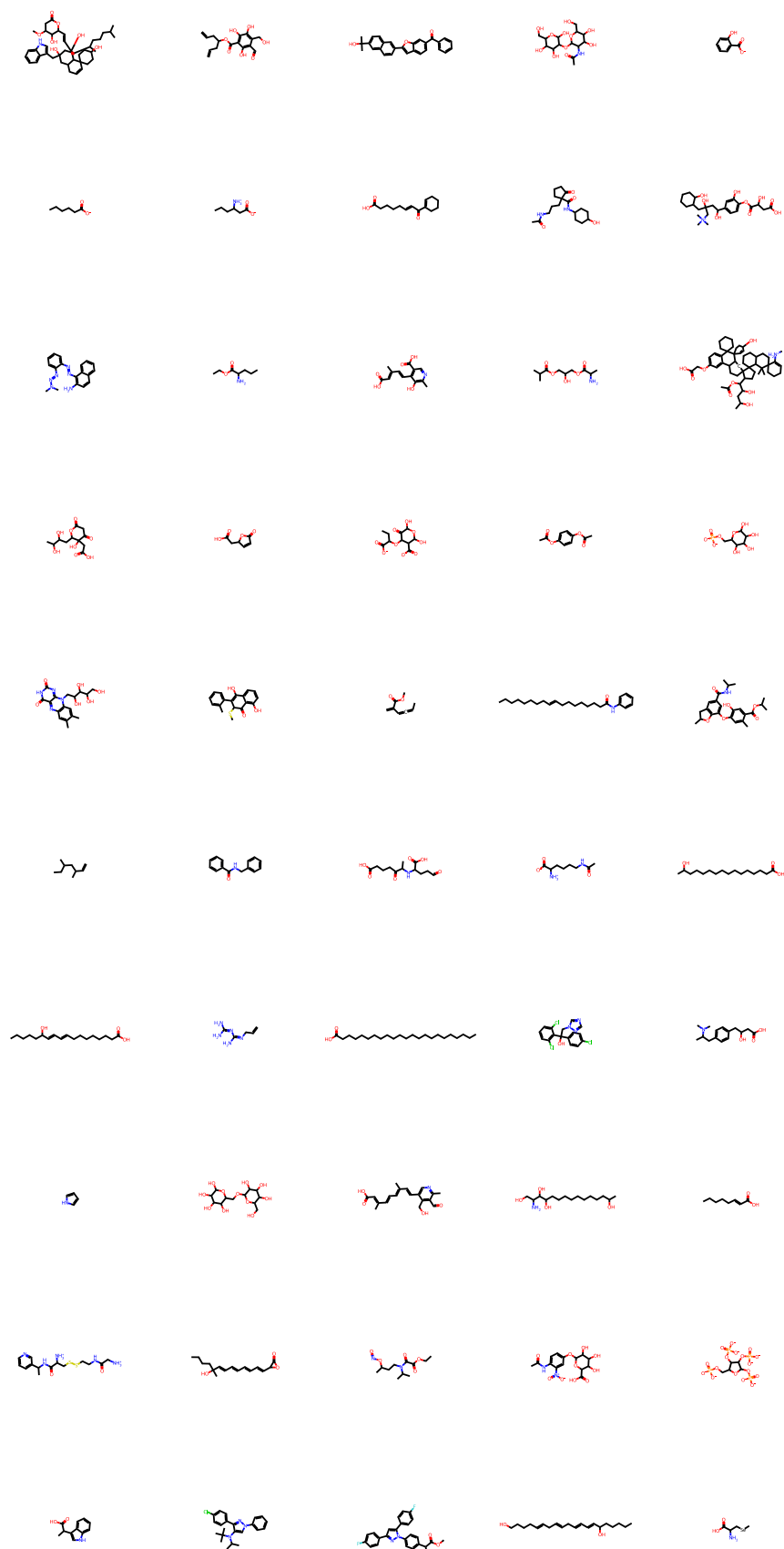


Figure 11. 50 molecules sampled from the prior distribution $\mathcal{N}(\mathbf{0}, \mathbf{I})$.